Journal of Statistical Physics, Vol. 64, Nos. 5/6, 1991

Interaction and Dynamics of Defects in Convective Roll Patterns of Anisotropic Fluids

Eberhard Bodenschatz,[1,2] Andreas Weber,[1] and Lorenz Kramer[1]

We present an overview of the dynamics and interaction of defects in roll patterns of electroconvection in nematic liquid crystals (EHC). For the decay of an Eckhaus-unstable pattern we distinguish three regimes, depending on the width of the system perpendicular to the wavenumber mismatch. Motivated by recent experiments, we examine the annihilation process of defects in patterns with wavenumber near to band center, where the motion of the defects is dominated by the interaction. The comparison with the experiments shows that this process can be described even quantitatively within the framework of Ginzburg–Landau theory.

KEY WORDS: Electroconvection; Eckhaus instability; Ginzburg–Landau equation; defects.

1. INTRODUCTION

In two-dimensionally extended, pattern-forming systems topological defects play an important roll in the wavelength selection process and in the transition to turbulence. Therefore a detailed investigation of the properties of defects is necessary for the understanding of these phenomena. In isotropic systems, like Rayleigh–Bénard convection in simple fluids, the convective rolls appear at threshold, in general, randomly oriented in the plane of the fluid layer, if not forced by boundary conditions (see, e.g., ref. 1). Thus, the pattern has many defects and grain boundaries that do not disappear within a reasonable time. Furthermore, in the vicinity of threshold, ordered periodic roll patterns with wavenumber q are subject to the zigzag instability,[1] which limits the band of stable solutions essentially

[1] Physikalisches Institut der Universität Bayreuth, Postfach 101251, 8580 Bayreuth, Germany.
[2] Present address: Physics Department, University of California at Santa Barbara, Santa Barbara, California 93106.

0022-4715/91/0900-1007$06.50/0

to $q > q_c$, where q_c is the critical wavenumber of the roll pattern appearing at threshold. This leads to the fact that the theoretical analysis of the dynamics of defects[2] and experimental results are not in satisfactory agreement.[3] For anisotropic fluids the situation is different. The axial anisotropy leads to a preferred orientation of the convective rolls and the zigzag instability is usually not present. Thus, two-dimensionally extended, well-ordered states can be achieved experimentally, which is necessary for the investigation of individual defects.

The most prominent example for a pattern-forming system with axial anisotropy is the electrohydrodynamic convection of planarly aligned nematic liquid crystals (EHC) (see, e.g., ref. 4). There the intrinsic axial anisotropy leads to convection rolls that are orientated normal or oblique to a preferred direction given by a prealignment of the molecules at the parallel glass plates confining the layer.[5] Due to the degeneracy of the angle of the oblique rolls with respect to the preferred axis, zigzag patterns may be found experimentally. Universal envelope equations describing the patterns in the vicinity of threshold were derived[6] and quantified from the hydrodynamic equations.[7-9] In the normal-roll case various theoretical results have been probed by experiment and good quantitative agreement has been found.[10] Some of the measured and compared properties are: the neutral curve for normal rolls, the coherence lengths and relaxation time,[10] the amplitude of convection,[11] the stability boundaries of the band of periodic solutions (Eckhaus instability),[12,13] the evolution of an unstable into a stable state and the dynamics and interaction of defects.[10,14,15]

It should be mentioned that some experimental results cannot be explained by the theoretical analysis of the standard electrohydrodynamic equations[7,9]: the bifurcation to traveling waves[4] and the very recent observation of a weak backward bifurcation to normal rolls.[16] On the other hand, the transition to weak turbulence, which is observed in experiment slightly above threshold, may be explained by mean-flow effects,[8] which are contained in the established electrohydrodynamic equations.

2. DYNAMICS AND INTERACTION OF DEFECTS

We confine ourselves to the region near threshold. Here a universal description in terms of complex envelope equations can be used.[6,7] The physical solutions and their slow space and time dependence can be written in the form

$$u_j = \varepsilon^{1/2}[A(X, Y, T)\, U_j e^{i(q_c x + p_c y)} + \text{c.c.}]\, w_j(z, t) + \mathcal{O}(\varepsilon) \qquad (1)$$

where $\varepsilon \ll 1$ measures the dimensionless distance from threshold, the functions w_j capture the z, t dependence of the linear modes at threshold, $A(X, Y, T)$ is a complex, slowly-varying function depending on the slow space and time variables

$$X = \varepsilon^{1/2} x, \qquad Y = \varepsilon^{1/2} y, \qquad T = \varepsilon t \tag{2}$$

and c.c. denotes the complex conjugate.

A perturbation expansion up to order $\varepsilon^{3/2}$ leads to a solvability condition for the complex envelope A,

$$T_0 \partial_T A = [\xi_1^2 \partial_X^2 + \xi_2^2 \partial_y^2 + 2\xi_1 \xi_2 a \partial_X \partial_Y + 1 - |A|^2] A \tag{3}$$

The linear part of this equation describes the neutral surface in parabolic approximation. Thus, the parameters ξ_1, ξ_2, and a can be calculated from the neutral surface and the relaxation time T_0 is obtained from the growth rate of the linear solutions. In the case of EHC the parameters were calculated for the material MBBA and can be found in refs. 7 and 8.

Equation (3) describes oblique rolls as well as normal rolls ($a = 0$), but it does not describe zigzag patterns, where oblique rolls with both orientations are present. In this case coupled equations similar to Eq. (3) have to be used.[9] Also in the vicinity of the Lifshitz point, where the oblique and normal roll regimes merge, a different envelope equation has to be used.[6,7] In this regime the system has some similarity to isotropic systems and the envelope equation is in fact a generalization of the well-known Newell–Whitehead equation.[17]

By rotation and scaling, Eq. (3) can be transformed into the more symmetric form

$$\partial_T A = [\partial_X^2 + \partial_Y^2 + 1 - |A|^2] A \tag{4}$$

This equation is identical to the time-dependent Ginzburg–Landau equation for superfluid ^{4}He.[18] It has stationary periodic solutions of the form

$$A = (1 - Q^2 - P^2)^{1/2} e^{i(QX + PY)} \tag{5}$$

which describe roll patterns above threshold with a wavevector[9,15]

$$\mathbf{q} = [q_c + \varepsilon^{1/2}(Q \cos\alpha/\xi_+ - P \sin\alpha/\xi_-),\ p_c + \varepsilon^{1/2}(Q \sin\alpha/\xi_+ + P \cos\alpha/\xi_-)] \tag{6}$$

where

$$\xi_{+/-}^2 = 1/2\{\xi_1^2 + \xi_2^2 \pm [(\xi_1^2 - \xi_2^2)^2 + 4a^2 \xi_1^2 \xi_2^2]^{1/2}\}$$

$$\tan(2\alpha) = 2a\xi_1 \xi_2 / (\xi_1^2 - \xi_2^2)$$

Linear stability analysis of the solution (5), (6) shows, that it is stable for $Q^2+P^2<Q_E^2=1/3$,[6] which is a direct generalization of the Eckhaus stability criterion known from quasi-one-dimensional systems.[19]

We now consider the decay of an unstable periodic pattern with $Q^2+P^2>1/3$. For simplicity we choose $P=0$. The general case is recovered by a simple rotation. One easily finds that the linear modes that destabilize the periodic solutions are given by

$$\delta A=[a_+ e^{i(KX+LY)}+a_- e^{-i(KX+LY)}]\, e^{\sigma T} \tag{7}$$

where the growth rate is

$$\sigma=-(1-Q^2)-K^2-L^2+[(1-Q^2)^2+4Q^2K^2]^{1/2} \tag{8}$$

The maximal growth rate for $Q^2>1/3$ is

$$\sigma_{\max}=(3Q^2-1)^2/4Q^2, \qquad K_{\max}^2=(3Q^2-1)(1+Q^2)/4Q^2, \qquad L_{\max}^2=0 \tag{9}$$

Expanding σ around $K_{\max}$ and $L_{\max}$ gives

$$\sigma=\sigma_{\max}[1-C_1^2(K-K_{\max})^2-C_2^2L^2] \tag{10}$$

$$C_1^2=(1+Q^2)/(3Q^2-1)\,Q^2, \qquad C_2^2=4Q^2/(3Q^2-1)^2 \tag{11}$$

C_1 and C_2 define (dimensionless) length scales which characterize the width of the modulation-wavevector spectrum (K, L) that can be expected to contribute to the initial destabilization process. For normal rolls the corresponding physical lengths are $\xi_x=C_1\xi_1\varepsilon^{-1/2}$ and. $\xi_y=C_2\xi_2\varepsilon^{-1/2}$. Assuming that the size of the system is sufficiently large in the X direction, we can now distinguish three regimes for the width L_y in the Y direction:

(i) $L_y\lesssim\xi_y$: Modes in the y direction are suppressed. The system behaves quasi-one-dimensionally and there the wavelength-changing process, which comprises creation or annihilation of roll pairs, has been discussed in some detail.[20] The system makes essentially one phase slip per modulation wavelength and ends in a periodic solution with final wavenumber near $|Q_f|=|Q|-|K_{\max}|$.

(ii) $L_Y\sim\xi_Y$: The situation is similar to (i) except that a phase-slip process is resolved into the creation of a defect pair, motion in y direction, and annihilation at the boundary (or equivalent). Simulations for this case have been presented.[21]

(iii) $L_Y\gg\xi_Y$: Then many defect pairs are created in the Y direction for every modulation wavelength. The system has now the chance to reach the most stable state $Q=0$ by creating/annihilating as many rolls as

necessary by defect motion and annihilation. One expects a smooth crossover from the case (ii) to (iii). Some detailed simulations are presented in ref. 22.

Note that, since ξ_Y diverges when $|Q| \to 1/3$ from above, even rather wide systems should in principle exhibit a crossover from cases (iii) to (ii) and (i) when Q approaches the stability boundary. It appears that the experiments by Rasenat *et al.*[13] were done in cases (i) and (ii), whereas those of Lowe and Gollub[12] pertain essentially to case (iii). This could explain why in the latter case the system actually ended up near the band center after a sufficiently long time.

In the following we will consider stable periodic states, where $Q^2 < Q_E^2$. All periodic states, except $Q=0$ (band center), are metastable. Evolution to the band center can occur by the motion of defects, once they have been nucleated by finite fluctuations or perturbations.[15] Mathematically a (point) defect is a (simple) zero of the complex amplitude A and can be characterized by a crossing of the lines $\mathrm{Re}(A)=0$ and $\mathrm{Im}(A)=0$. Near the center one has $A \sim (X+iY)$ and therefore A is perfectly analytical. There are two types of zeros with opposite polarity. The phase either increases or decreases by 2π when encircling the zero in a clockwise sense. One therefore can associate "topological charges" $+1$ or -1 with the defects. In the bulk, defects can only be nucleated (by finite fluctuations in the stable range) or annihilated in pairs. The homogeneous nucleation of defects has been considered in ref. 15.

By using Eq. (4), the velocity V of isolated defects was calculated analytically in the limit $Q^2 \ll 1$, leading to $V \ln(3.29/V) = 2Q$ for a sufficiently large system,[15] as well as numerically in the whole region $0 < Q < Q_E$.[14,9] The results can be described to high accuracy by the formula $V \ln(3.29/V) = 2Q(1-0.35Q^2)$. The motion of an isolated defect is always perpendicular to $\mathbf{Q}$. The force on the defect is similar to a Peach–Koehler force on defects in solids. Behind a defect the wavenumber of the pattern is changed by $2\pi/L$, where L is the size of the system. Thus, the pattern is brought nearer to the band center $Q=0$, where the velocity V of an isolated defect is zero. A comparison of our results with recent experiments shows good quantitative agreement.[10,14]

The interaction and annihilation of defects is also described by Eq. (4). The analysis of an isolated, moving dislocation shows that the deformation of the roll pattern decays in front exponentially over a distance $R = 1/V$, while behind the dislocation the decay is proportional to $R^{-1/2}$ [see, e.g., Eq. (2.17) of ref. 15]. Thus, if the background wavenumber Q is nonzero and two defects with opposite topological charge are approaching each other, the velocity will be constant for $R \gtrsim 2/V \sim 2/Q$. Subsequently the

motion will accelerate and eventually the attraction will dominate over the Peach–Koehler force and lead to annihilation. This can be seen in simulations.[9]

In recent experiments by Braun and Steinberg this annihilation process was studied in detail for situations near band center ($Q \ll 1$) where a determination of Q was not possible.[23] To make a quantitative comparison we have conducted further simulations of Eq. (4). In Fig. 1 the distance L between two defects of opposite polarity approaching each other along a straight line is plotted versus time T for different Q in scaled units. At $T=0$ the defects annihilate. The solid lines give the numerical results and the squares, circles, and diamonds are experimental results for climb motion (see figure caption for details).

The case $Q=0$, where the Peach–Koehler force vanishes so that $V \to 0$ for $L \to \infty$, deserves special attention. The analysis in ref. 15 then leads to $VL=2/C$, where $C \approx \ln(L/2.26)$ for $L \gg 1$ and $VL \ll 1$. Computationally, it is very difficult to verify the logarithmic dependance of C on L because of finite-size effects which influence the results strongly when $L \gg 1$. For small distances, shortly before annihilation, the gradient terms in the Ginzburg–Landau equation presumably become dominant and one may argue that the dynamics is governed by a self-similar solution of the diffusion equation so that $L \sim T^{1/2}$,[24] which appears consistent with the numerical results.

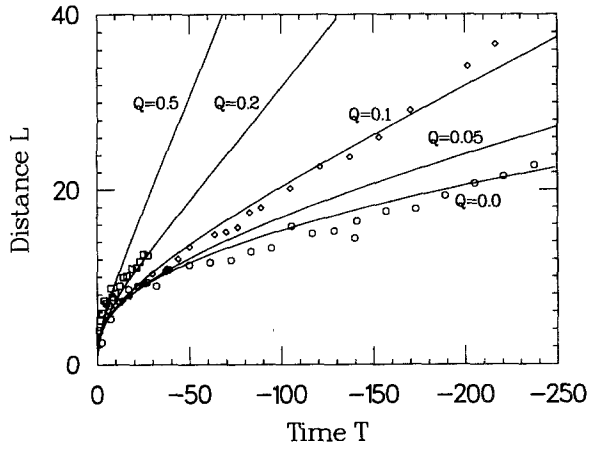

Fig. 1. The distance L between two defects of opposite polarity that approach each other on a straight line is plotted for different background wavenumbers Q versus time T (reduced units). For comparison the experimental results of Braun and Steinberg are included. The different symbols denote different distances ε from the threshold (circles: $\varepsilon=0.02$; squares: $\varepsilon=0.04$; diamonds: $\varepsilon=0.005$) (see Fig. 1 of ref. 23). The point $T=0$ marks the annihilation of the defects.

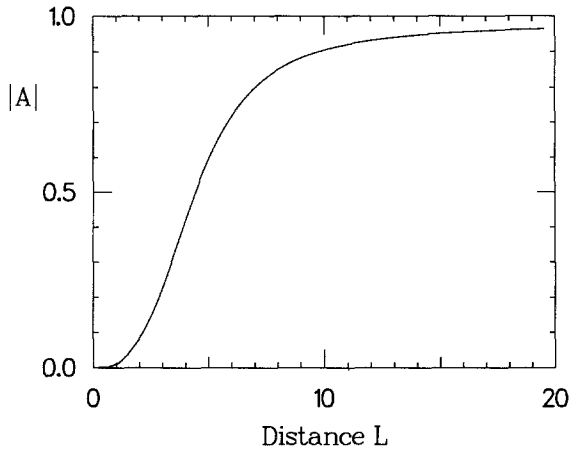

Fig. 2. The maximum of $|A|$ along the connection line of the defect centers is plotted versus the distance L of the defects. For distances smaller than about $L=8$, $|A|$ starts to decrease significantly, marking the onset of overlap of the defect cores.

Allowing for a small wavevector displacement Q, one finds $V(L+1/Q)=2/C$, where C is the same as above if $VL \gg 1$. One now can also have the opposite limit $VL \ll 1$ and then, for a sufficiently large system, $C=\ln(3.29/V)$. Note that when interaction and Peach–Koehler force oppose each other one has (unstable) equilibrium at $L=1/Q$.[15]

In Fig. 1 the agreement with experiments seems to be reasonable if one allows for values of Q up to 0.2. The authors of ref. 23 argue that there is a break in the velocity curves around $L_s \approx 7$–8 signaling the existence of a second length scale. We wish to point out that our simulations for $Q \ll 1$ exhibit such kind of a crossover which can be explained by the fact that around L_s the overlap of the dislocation cores becomes significant, leading to substantial distortion of $|A|$. This is seen from Fig. 2, where we plot the maximum of $|A|$ along the line connecting the defect centers. $|A|$ starts to decrease strongly around L_s.

When two dislocations approach each other in a situation where the Peach–Koehler force is not along the line which connects the defects, the defects can encircle each other up to 180 deg before annihilation. This effect has also been observed in experiments.[25]

3. CONCLUDING REMARKS

We have given an overview of the investigation of defects in patterns of anisotropic fluids. It is shown that the motion, interaction, and annihila-

tion of defects near threshold can be described even quantitatively within the framework of the Ginzburg–Landau equation. Nonadiabatic effects which couple the glide of a defect to the underlying roll pattern are not included. As long as the experiment is conducted not too near to the transition to weak turbulence, mean-flow effects seem not to play a significant roll for the dynamics of defects. Otherwise a modified version of envelope equations has to be used.[8]

ACKNOWLEDGMENTS

We would like to thank W. Pesch for useful discussions. This work has been supported by Deutsche Forschungsgemeinschaft SFB 213, Fonds der chemischen Industrie, and Emil Warburg Stiftung Bayreuth.

REFERENCES

1. F. H. Busse, *Rep. Prog. Phys.* **41**:28 (1978); and in *Hydrodynamic Instabilities and the Transition to Turbulence*, 2nd ed., H. L. Swinney and J. P. Gollub, eds. (Springer, Berlin, 1986).
2. E. D. Sigga and A. Zippelius, *Phys. Rev. A* **24**:1036 (1981).
3. A. Pocheau and V. Croquette, *J. Phys. (Paris)* **45**:35 (1984).
4. I. Rehberg, B. L. Winkler, M. de la Torre Juarez, S. Rasenat, and W. Schöpf, in *Festkörperprobleme/Advances in Solid State Physics*, Vol. 29, U. Roessler, ed. (Vieweg, Braunschweig, 1989); A. Joets and R. Ribotta, *Phys. Rev. Lett.* **60**:2164 (1988); I. Rehberg, S. Rasenat, and V. Steinberg, *Phys. Rev. Lett.* **62**:756 (1989); S. Kai, N. Chizumi, and M. Kohno, *Phys. Rev. A* **40**:6554 (1989).
5. A. Joets and R. Ribotta, in *Cellular Structures in Instabilities*, J. E. Wesfreid and S. Zaleski, eds. (Springer, Berlin, 1984); W. Zimmermann and L. Kramer, *Phys. Rev. Lett.* **55**:2655 (1986).
6. W. Pesch and L. Kramer, *Z. Phys. B* **63**:121 (1986).
7. E. Bodenschatz, W. Zimmermann, and L. Kramer, *J. Phys.* **49**:1875 (1988).
8. M. Kaiser, W. Pesch, and E. Bodenschatz, submitted to *Physica D* (1990); and in preparation.
9. L. Kramer, E. Bodenschatz, W. Pesch, W. Thom, and W. Zimmermann, *Liq. Cryst.* **4**:699 (1989).
10. S. Rasenat, I. Rehberg, and V. Steinberg, submitted to *Phys. Rev. A*.
11. S. Rasenat, G. Hartung, B. L. Winkler, and I. Rehberg, *Exp. Fluids* **7**:412 (1989).
12. M. Lowe and J. P. Gollub, *Phys. Rev. Lett.* **55**:2575 (1985).
13. S. Rasenat, E. Braun, and V. Steinberg, preprint (1990).
14. L. Kramer, E. Bodenschatz, and W. Pesch, *Phys. Rev. Lett.* **64**:2588 (1990).
15. E. Bodenschatz, W. Pesch, and L. Kramer, *Physica D* **32**:135 (1988).
16. I. Rehberg, S. Rasenat, M. de la Torre, W. Schöpf, F. Hörner, G. Ahlers, and H. R. Brand, to be published.
17. A. C. Newell and J. A. Whitehead, *J. Fluid Mech.* **38**:279 (1969).
18. V. L. Ginzburg and L. Pitaevskii, *Zh. Exp. Teor. Fiz.* **34**:1240 (1958) [English transl.: *Sov. Phys. JETP* **7**:858 (1958)].

19. W. Eckhaus, *Studies in Nonlinear Stability Theory* (Springer, Berlin, 1965), pp. 63ff.
20. L. Kramer, H. Schober, and W. Zimmermann, *Physica D* **31**:212 (1988).
21. E. Bodenschatz, M. Kaiser, L. Kramer, W. Pesch, A. Weber, and W. Zimmermann, in *New Trends in Nonlinear Dynamics and Pattern Forming Phenomena: The Geometry of Non-equilibrium*, P. Coullet and P. Huerre, eds. (Plenum Press, New York, 1990).
22. E. Bodenschatz, Doctoral Dissertation, Bayreuth (1989).
23. E. Braun and V. Steinberg, *Europhys. Lett.* **15**:167 (1991).
24. I. Aranson, private communication.
25. S. Nasuno, S. Takeuchi, and Y. Sawada, *Phys. Rev. A* **40**:3457 (1989).